Localization of magnetic pills

Bryan Laulicht[a,1], Nicholas J. Gidmark[b], Anubhav Tripathi[c], and Edith Mathiowitz[a,c,2]

[a]Department of Molecular Pharmacology, Physiology, and Biotechnology; [b]Department of Ecology and Evolutionary Biology; and [c]Division of Engineering and Medical Science, Brown University, Providence, RI 02912

Edited* by Robert Langer, Massachusetts Institute of Technology, Cambridge, MA, and approved December 15, 2010 (received for review November 3, 2010)

Numerous therapeutics demonstrate optimal absorption or activity at specific sites in the gastrointestinal (GI) tract. Yet, safe, effective pill retention within a desired region of the GI remains an elusive goal. We report a safe, effective method for localizing magnetic pills. To ensure safety and efficacy, we monitor and regulate attractive forces between a magnetic pill and an external magnet, while visualizing internal dose motion in real time using biplanar videofluoroscopy. Real-time monitoring yields direct visual confirmation of localization completely noninvasively, providing a platform for investigating the therapeutic benefits imparted by localized oral delivery of new and existing drugs. Additionally, we report the in vitro measurements and calculations that enabled prediction of successful magnetic localization in the rat small intestines for 12 h. The designed system for predicting and achieving successful magnetic localization can readily be applied to any area of the GI tract within any species, including humans. The described system represents a significant step forward in the ability to localize magnetic pills safely and effectively anywhere within the GI tract. What our magnetic pill localization strategy adds to the state of the art, if used as an oral drug delivery system, is the ability to monitor the force exerted by the pill on the tissue and to locate the magnetic pill within the test subject all in real time. This advance ensures both safety and efficacy of magnetic localization during the potential oral administration of any magnetic pill-based delivery system.

magnetic pills | retention | localization | drug delivery

For many orally administered pharmaceuticals, increased residence time in a particular region of the gastrointestinal (GI) tract would greatly improve their therapeutic benefit (1–3). Typically, physiological digestive processes govern the GI residence of standard pills. We have developed a magnet-based delivery system visualized by biplanar videofluoroscopy in vivo that yields real-time monitoring and control over the duration of GI residence of model magnetic pills in the small intestines of rats both as a tool for investigating the GI site-specific absorption and action of therapeutics and as a critical step towards enabling clinical localization of magnetic pills. Our system can safely and reliably retain drugs for a user-defined duration in any region of the GI with the ability to monitor and control the force applied by the orally ingested magnet to the intestinal wall. Because duration of retention is user-defined unlike standard pills, it can be adjusted to match drug release kinetics in the area of greatest absorption or therapeutic action without altering the formulation.

What our approach to GI retention adds to previous systems is the ability to visually confirm the anatomical location of the oral dose and to constantly monitor and regulate the intermagnetic force ensuring safe localization of the oral dosage in the appropriate region of the GI (2–9). Previous studies have used static external magnets, without any means of intermagnetic force monitoring or real-time feedback confirming localization, to improve the bioavailability of orally administered proteins including insulin for diabetics (4, 5, 10), narrow absorption window (NAW) therapeutics including acyclovir as an antiviral therapy (1, 3), and therapeutics for site-specific pathologies including bleomycin for esophageal cancer (7). Diseases and disorders of the GI represent a substantial worldwide health burden. The World Health Organization reports that stomach and colorectal cancer alone caused more than 1.4 million deaths in 2009, 803,000 and 639,000 respectively (11). Other site-specific GI diseases and disorders caused 13.5 million hospitalizations in 2004 in the United States, for example severe Crohn's disease accounted for 141,000 hospitalizations (12). Localized drug delivery within the GI would greatly benefit the treatment of diseases and disorders, such as digestive cancers and severe Crohn's disease, that exhibit site-specific GI pathophysiology.

In all previous studies, the magnet was applied in a fixed position without measuring intermagnetic force or visually confirming the localization of the oral dosage, thereby requiring post hoc indirect measures of safety and efficacy (2–9). Our system conveys real-time, direct confirmation of localization both with real-time intermagnetic force monitoring and with biplanar videofluoroscopy. Unlike prior studies, our system monitors force applied by the orally administered magnetic pill via a load-cell in series with the external magnet and its anatomic location visualized by biplanar fluoroscopy in the GI ensuring safety and efficacy of extended localization at a site of therapeutic interest. Though not previously tractable, it is believed that localized oral drug delivery potentiates significant therapeutic benefit for oral delivery of therapeutics for severe inflammatory bowel disease to the colon (1), of orally administered chemotherapeutics to digestive cancers (7, 9, 13), and of oral vaccines to the gut-associated lympoid tissue (GALT) in the ileum (14). The described magnetic localization platform enables investigation of the benefits of localized as compared to systemic administration of therapeutics.

Early GI magnetic retentive efforts for oral administration focused on creating the maximal attractive force between a dosage and an external magnet to either retain a large dosage form at the site of interest (1, 3) or to increase the uptake of magnetic nanoparticle formulations (6, 14–19). We institute a computer-controlled material testing device equipped with a load-cell that has a programmed feedback loop, constantly adjusting the position of the external magnet between upper and lower intermagnetic force bounds defined by the user. As a result, we ensure that the GI tissue experiences the least amount of force possible that still retains the magnetic oral dose. Magnetic localization prolongs intimate contact between the dose and the absorptive GI epithelium promoting uptake and bioavailability without damaging intestinal tissue while providing visual confirmation of localization and quantitative force-sensing feedback in real time.

Results and Discussion

Each magnetic pill was administered by oral gavage to male, albino Sprague-Dawley rats prior to physical restraint. After the dosed magnet entered the small intestines, the restrained rat is placed on a modified materials testing device without anesthe-

Author contributions: B.L., N.J.G., and E.M. designed research; B.L. and N.J.G. performed research; B.L., N.J.G., A.T., and E.M. contributed new reagents/analytic tools; B.L., N.J.G., A.T., and E.M. analyzed data; and B.L., N.J.G., A.T., and E.M. wrote the paper.

The authors declare no conflict of interest.

*This Direct Submission article had a prearranged editor.

[1]Present address: Harvard-MIT Division of Health Sciences and Technology, Cambridge, MA 02139.

[2]To whom correspondence should be addressed. E-mail: Edith_Mathiowitz@Brown.edu.

This article contains supporting information online at www.pnas.org/lookup/suppl/doi:10.1073/pnas.1016367108/-/DCSupplemental.

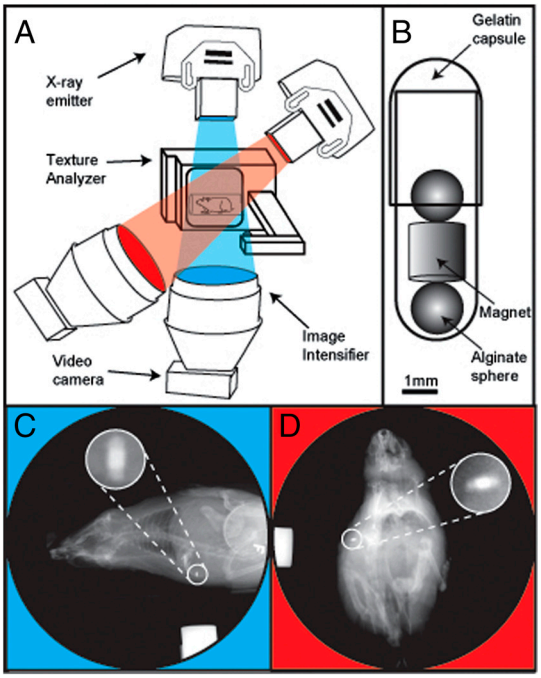

Fig. 1. Biplanar videofluorscopic tracking of magnetically retained model pills in vivo. (*A*) Schematic of setup for retaining magnetic pills within rat intestines visualized by biplanar fluoroscopy. (*B*) Drawing to scale of the localized magnetic pill. (*C* and *D*) Still images acquired from biplanar fluoroscopic videos showing magnetic model pill localization for 12 h due to the cyclic application of an external magnetic force. Insets highlight magnified views of the magnetic model pill with red and blue colored backgrounds corresponding to the fluoroscope emitters and detectors diagrammed in *A*. Each inset shows a radiopaque cylindrical NIB magnet with less radiopaque iron-loaded alginate beads on either end, localized in the small intestines.

sia (Fig. 1*A*). To achieve magnetic retention, a cylindrical neodymium iron boron (NIB) magnet ($\Phi = 25$ mm, length $= 25$ mm) is brought towards the subject until a maximal force of 4 mN is achieved. Upon reaching the maximum desired force, the external magnet retreats from the subject until a minimal force of 1 mN is reached. The cycle repeats with the external magnet moving at 0.5 mm/s for 12 h thereby localizing the magnetic pill, while regulating the force applied to the internal magnet and underlying tissue. Periodically releasing the intermagnetic force every 5–30 s, by force cycling, relieves tissue compression from impinging on vascular flow and releases tension on the mesenteric tissue between periods of maximal intermagnetic force.

The internal magnet is a cylindrical NIB magnet ($\Phi = 1.6$ mm, length $= 1.6$ mm) coated first in chrome, then nonerodible polymethyl methacrylate to protect the magnet from degradation within the GI. On both planar surfaces of the internal magnet, a freeze-dried calcium alginate sphere containing magnetic, radiopaque iron oxide microparticles was held in place by the magnetic attractive forces to create a model magnetic pill as diagrammed in Fig. 1*B*. In testing, placing any more than one sphere on each end without additional adhesives led to dissociation of the added spheres from the internal magnet upon gastric emptying. We chose to use alginate spheres because they can readily be loaded with magnetic microparticles while preserving the bioactivity of sensitive therapeutics (20); however, any drug delivery device that can be affixed to or contain the internal magnet, including standard tablets and capsules, could alternatively be used.

Due to the radiopacity of NIB, we were able to track the positions of both the internal and external magnets using fluoroscopy. To visualize the anatomical location and quantify external magnet induced motion of the internal magnet, biplanar fluoroscopic videos were recorded at prescribed time points (at the first instance of localization, 1, 2, 4, 8, and 12 h thereafter, an excerpt of which is provided in Movie S1). Exemplary X-ray images from orthogonally oriented fluoroscopy videos showing the magnetic dosage in the small intestines, with coadministration of aqueous barium sulfate to provide contrast in the surrounding GI lumen, are shown in Fig. 1 *C* and *D* (21). Due to the radiopacity of NIB, we were able to track the three-dimensional position of the internal magnet over time without additional markers (22). A two-dimensional projection of the motion of the internal magnet is plotted in blue in Fig. 2*A*. Motion arising from breathing artifacts were filtered by applying a 0.5 Hz low-pass filter yielding internal magnetic motion that correlates with cycling intermagnetic force plotted in red in Fig. 2*A* (a close-up fluoroscopic video of force cycling without breathing artifact in a post mortem rat is provided in Movie 2).

Three-dimensional motion of the frequency filtered internal magnet over the course of an exemplary force cycle is plotted in Fig. 2*B*. From proper orthogonal decomposition, we calculate that $98.2 \pm 1.8\%$ of the three-dimensional motion of the pill can be described by a single axis ($N = 5$), termed mode 1 (23). By taking the slope of the intermagnetic force as a function of position along mode 1, we calculated the restoring force experienced by the internal magnet in response to applied load (Fig. 3 *A* and *B*). The measured elasticity coefficients (k-values) ranged from 0.05–0.3 mN/mm, which is ~1–6% of the elasticity coefficient of a $0.7 \times 1.5 \times 155$ mm rubber band (Fig. 3*C*). Such low measured k-values indicate that the loop of intestine surrounding the localized magnetic pill moved relatively freely in response to applied load rather than undergoing significant compression.

Effectiveness and reproducibility of real-time force monitoring magnetic localization for 12 h was confirmed in three addi-

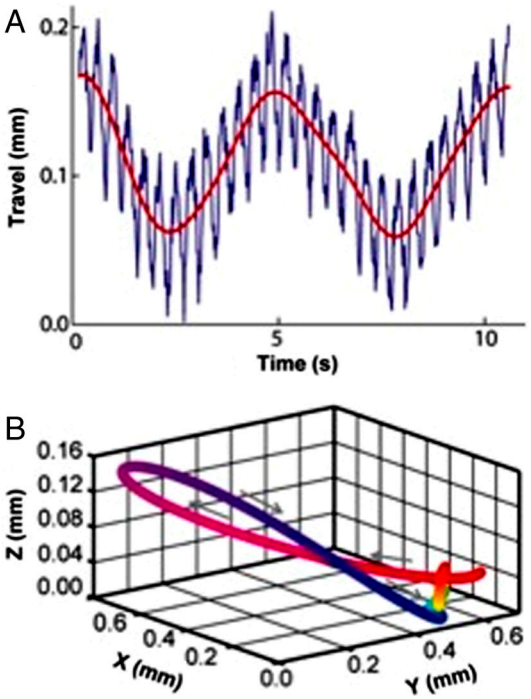

Fig. 2. Exemplary two-dimensional lateral trajectory plot of the raw data acquired by pill tracking in biplanar fluoroscopic videos before (blue) and after (red) filtering to remove motion unrelated to changes in intermagnetic forces. (*B*) Exemplary three-dimensional trajectory plot of a model magnetic pill moving in response to a single force cycle of the external magnet after filtering. Gray arrows point along the trajectory in the direction of increasing time.

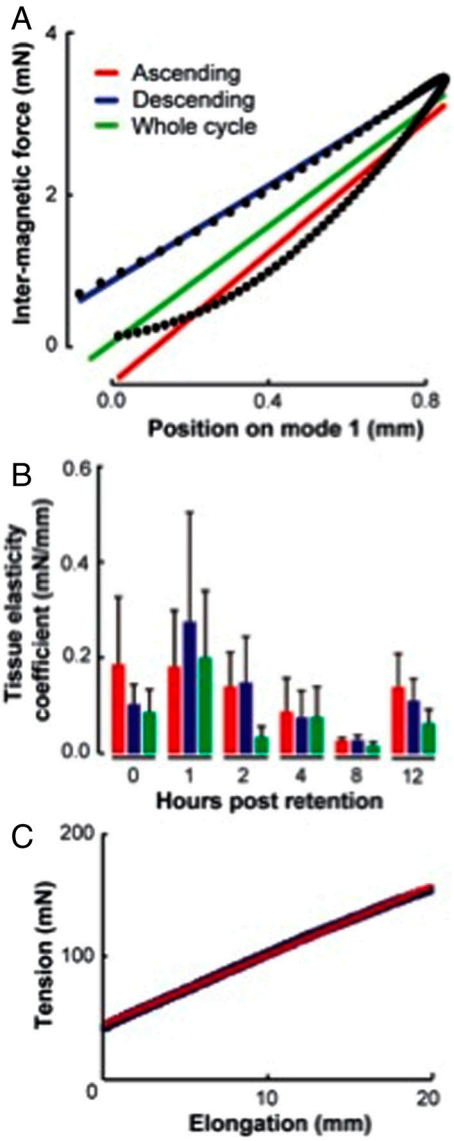

Fig. 3. In vitro/in vivo comparison of Hookean elasticity constants. (*A*) Exemplary intermagnetic force plotted as a function of travel along mode 1. Slopes of the best-fit lines to the ascending, descending, and whole cycle *k*-values of the internal magnet are the effective elastic constants of the intestinal tissue in response to force cycling. Observed hysteresis in the inter force-travel curve corresponds to the viscoelastic properties of the tissue. (*B*) Tissue elastic constant plotted as a function of time after the start of magnetic retention ($N = 5$) showing that there is no significant change ($P_{asc} = 0.52$, $P_{des} = 0.68$, and $P_{wc} = 0.48$) in tissue elasticity during 12 h of magnetic retention, indicating negligible change in the tissue restoring force during magnetic localization. Error bars represent SEM. (*C*) Tensile test results of a $0.7 \times 1.5 \times 155$ mm rubber band performed on the TA with a stretch rate of 1 mm/s providing a physical basis of comparison for in vivo measured *k*-values reported in *B*. The best-fit line (red) has a slope of 5.62 mN/mm, ~20–100× the elasticity constants measured in vivo, and demonstrates the high degree of linearity associated with natural rubber ($R^2 = 0.9991$).

tional subjects by standard X-ray (Fig. 4*A*). Future studies, especially in other nonrodent species such as humans that will not require confinement, may continue localization beyond 12 h in accordance with the standards of care for those subjects. In all cases, the magnet remained localized within the jejunum for the full 12 h as compared to control subjects ($N = 3$), which excreted orally gavaged magnets in the same period of time (Fig. S1). In contrast, without an external magnet none of the rats had dosages within the small intestines 12 h after administration. Evidencing the effectiveness of prolonged retention, the total GI residence time of the control pills was shorter than the residence of magnetically localized pills in specific regions of the small intestines. As an additional verification of the intermagnetic force monitoring system, when the entire rat is removed from the modified materials testing device, the intermagnetic force measurement drops to zero instantaneously, reporting the loss of magnetic localization to the investigator in real time. Due to the slow mean velocity of pill intestinal transit (2 cm/ min in the rat jejunum) and the length of the rat jejunum (~100 cm), we observed that the external magnet can be removed for up to ~1 h and reintroduced before the dose has progressed into the next segment of the GI (24). At the culmination of 12 h of localization, three subjects were killed to compare intestinal tissue samples in the region of localization (Fig. 4*B*) with control tissue samples 2 cm distal (Fig. 4*C*). Histological analysis post mortem confirmed that no signs of damage or inflammation were caused by retention. In addition to the safety of the mechanical aspects of localization, the magnetic fields produced by the NIB magnets used in this study, up to 2T, are classified as nonsignificant risk devices by the FDA (6).

To quantify the net inertial force experienced by the internal magnet, the portion of the intermagnetic force that causes acceleration of the internal magnet, we calculated its instantaneous acceleration from three-dimensional position as a function of time coordinates obtained from orthogonal biplanar fluoroscopic videos (Fig. 5*A*) using methods described previously (25, 26). Because the calculated peak inertial net force is only 0.0015± 0.0005% of the measured peak intermagnetic force, the intermagnetic force closely approximates the force the magnet applies to the GI tissue. Previous investigations demonstrated GI tissues have a mechanical stress threshold, ≥120 kPa in the porcine small intestine, that when exceeded causes inflammation and increased localized apoptosis (27). To ensure that the stresses applied by the internal magnet to the underlying tissue were within a safe range, the 1–4 mN intermagnetic force experienced by the tissue was normalized by the 2 mm^2 cross-sectional area of contact with the magnetic pill yielding localized stress of 0.5–2 kPa. The local stress imparted by magnetic pill localization corresponds to pressures ranging from 4–16 mmHg indicating that pressures experienced by the tissue during retention are within the normal physiological range for rat jejunal tissue (28). Pressures experienced by the GI region of interest are excellent guidelines for the range of safe tissue stresses imparted by localization of a magnetic pill because the tissue is naturally exposed to pressure cycling in that range (28).

In order to provide a quantitative in vitro test for choosing a pair of external and internal magnets that will achieve sufficient force at a physiologically relevant distance to localize a dose, we compared intermagnetic force as a function of intermagnetic distance in vitro with in vivo measurements (Fig. 5*B*). Because the presence of a live subject makes a negligible difference in intermagnetic attractive strength, internal and external magnet size and strength selected based on in vitro force as a function of intermagnetic separation testing will translate seamlessly into in vivo studies. As such, given readily quantifiable parameters including the lateral dimensions of the experimental subject, the intermagnetic force ($\vec{F}_{mag}$), and the GI propulsive net force in the region of retention ($\vec{F}_{net}$), localization efficacy can be evaluated in vitro prior to live subject studies in any region of the GI of any species. If the intermagnetic force measured at the physiologically relevant distance between the nearest external cutaneous surface of the subject and the internal magnet (ΔS_{I-M}) is greater than the maximal propulsive net force in the region, estimated by analyzing the net inertial force from high resolution magnetic pill tracking data (25, 26), magnetic capture can be

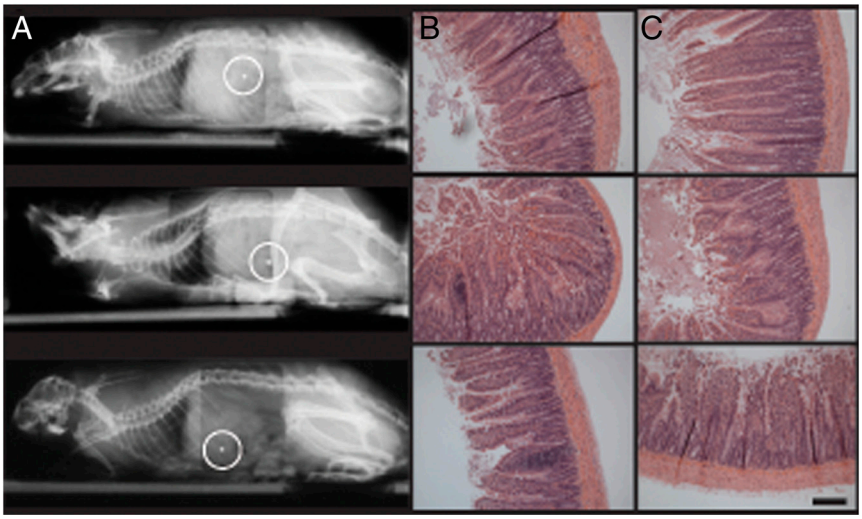

Fig. 4. Confirmation of magnetic localization efficacy by X-ray, and safety by histology. (*A*) X-ray confirmation of magnetic pill retention in the small intestines of rats ($N = 6$) demonstrating the efficacy of magnetic retention. Orally administered magnets are circled in white. (*B*) Bright field micrographs of hemotoxylin and eosin stained segments of the small intestines in the region of magnetic localization for 12 h (experimental) and (*C*) distal to that region (control). All images were acquired at 100× magnification and the scale bar on the bottom right represents 200 microns. There is no observable difference among the intestinal sections demonstrating that magnetic retention does not cause inflammation or necrosis.

expected for any species including humans. Given the force threshold below which tissue viability remains unchanged ($\vec{F}_{\max}$), the conditions for safe and effective magnetic pill localization are:

$$\vec{F}_{\max} \geq \vec{F}(\Delta S_{I-M}) \geq \vec{F}_{\text{net}}.$$

Monitoring and regulating a cyclically applied intermagnetic force between a magnetic oral dose and an external magnet enabled the safe and effective localization of a model pill. Magnetic force monitoring reports the intermagnetic force in real time, while biplanar X-ray fluoroscopy with contrast enables quantitative verification of the intermagnetic distance and anatomic location in vivo in real time. Together, intermagnetic force monitoring and biplanar fluoroscopic visualization provide a means for localizing oral drug delivery systems with quantitative means of assessing safety and efficacy.

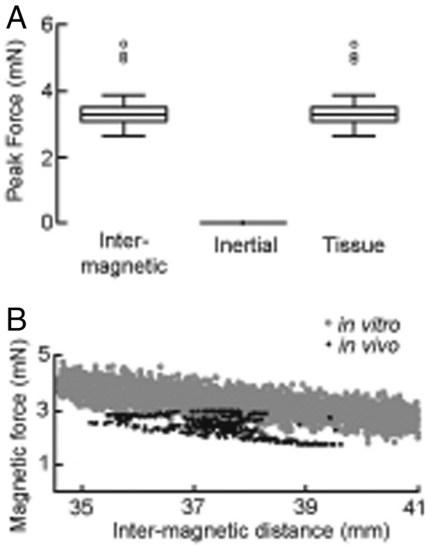

Fig. 5. (*A*) Comparison of median peak "intermagnetic", net "inertial", and "tissue" forces ($N = 5$) showing that a negligible fraction ($0.0015 \pm 0.0005\%$) of intermagnetic force translates into net inertial force demonstrating that the measured intermagnetic force is a good approximation of the force imparted by the internal magnet upon the underlying intestinal tissue. Error bars represent SEM. (*B*) Comparison plot of intermagnetic force as a function of intermagnetic distance in vitro and in vivo showing minimal differences enabling the accurate prediction of magnetic pill localization in vitro for use in choosing the appropriate magnet pair for achieving localized drug delivery in any region of the GI in any species.

Additionally, combining datasets from in vitro intermagnetic force as a function of distance testing, in vivo tracking-based calculation of forces experienced by a magnetic pill, and local manometric measurements of GI pressure experienced during digestion, provide quantitative selection criteria for magnet pairings that will safely and effectively achieve localization of a magnetic pill in any species. At present we show that the technology provides an experimental tool for animal studies; however, we carefully characterized the intermagnetic forces in vitro and in vivo towards providing a means of translating the system among species and ultimately finding use as a clinical tool in humans. While we ultimately hope that the safety and efficacy of the magnetic localization technique could be used in an outpatient setting, the technique can immediately be very useful in research and development of therapies involving local delivery of drugs in the GI tract and with further development for inpatient applications.

Materials and Methods

Magnetic Pill Preparation. Orally administered magnetic pills consist of two freeze-dried alginate spheres on either side of a NIB magnet ($\Phi = 1.6$ mm, length $= 1.6$ mm, KJ Magnetics). The alginate spheres were created by introducing 30 weight per volume % iron microparticles (Sigma-Aldrich) suspended in an aqueous 2 weight per volume% low viscosity sodium alginate (Sigma-Aldrich) into an aqueous 1 weight per volume% calcium chloride (Sigma-Aldrich) receiving bath. The sodium alginate solution was extruded through a 21-gauge syringe needle at 3 mL/min by a vertically oriented syringe pump (Harvard Apparatus). Upon entering the receiving bath, the divalent cationic calcium ionically cross-links the polyanionic alginate as described previously (13). The alginate spheres are collected, rinsed with distilled water and then freeze dried overnight. Once the doses are assembled, they are loaded into size 9 gelatin capsules (Torpac) for oral gavage. Coadministration of a radiopaque contrast agent can elucidate more precisely the anatomical position of the magnet at the cost of magnet localization precision. Although magnetic alginate spheres are suitable for delivering numerous therapeutics in a controlled fashion, any dosage form that yields sufficient intermagnetic strength for retention could be used.

Force Monitoring of Magnetic Localization. A texture analyzer XT-plus (Texture Technologies) was modified to hold a rat in an acrylic restraint tube on its base while the load-cell-containing arm is oriented to move horizontally. The texture analyzer was programmed using Texture Exponent Software (Texture Technologies) to begin its cycle 50 mm from the outer surface of the acrylic restraint tube and to approach the tube at 0.5 mm/s until a force of 4 mN is reached. Upon reaching an intermagnetic tensile force of 4 mN, the arm moves away from the rat at constant speed until a minimal force of 1 mN is reached. The cycle, which takes approximately 30 s, repeats for a user-defined period. Force cycling allows for the intermittent release of retaining force to ensure minimal tissue damage. Real-time intermagnetic force monitoring the force ensures that the internal magnet does not apply any undue stress to the GI tissue.

Biplanar Videofluoroscopic Spatial Calibration, Visualization, Tracking, and Analysis of Magnet Motion. C-arm fluoroscopes (OEC Model 9400) were retrofitted with 30 cm Image Intensifiers (Dunlee model TH9432HX, Dunlee Inc.) and Photron video cameras (Fastcam 1024 PCI, Photron, Inc.). Algorithms to account for distortion introduced by the fluoroscopes and to determine their three-dimensional positions were executed in MATLAB (The Mathworks) using custom software and a 64-point calibration cube (15). We used MATLAB scripts embedded in XrayProject version 2.0.7, available for download at http://www.xromm.org. Marker tracking scripts, embedded within XrayProject version 2.0.7 were used in calculating three-dimensional positions of the internal magnet and the external arm (15, 16). We used a 0.5 Hz low-pass filter to remove noise introduced by breathing artifact that appears as a low frequency wave because of interference introduced because it occurs on the order of frame capture rate (60 Hz) to arrive at the internal magnet's three-dimensional coordinates.

Motion of the internal magnet was primarily along a single line [the line of motion of the Texture Analyzer (TA) arm]. We tracked movement in world space, but this line of action of the TA arm was not precisely contained within either the *x*, *y*, or *z* dimension of our calibration cube. To reduce this dimensionality, we used Proper Orthogonal Decomposition. Mathematically, this technique is identical to Principal Components Analysis or Singular Value Decomposition, transforming three-dimensional coordinate space such that one axis (herein termed mode 1) explains the greatest possible amount of variation in the data (17). Given three parameters (*x*, *y*, and *z* coordinates, in cube space, over time), our dataset has three modes. Mode 1 explained $98.2 \pm 1.8\%$ of variation in position over time, so we used the position along mode 1 as an approximation of movement of the internal magnet. Similar analyses were performed on the position of the TA arm, where mode 1 explained $98.6 \pm 1.3\%$ of the variation.

Force recordings from the Texture Analyzer were synchronized with recordings from the videofluoroscopy by comparing the TA arm position (as measured by the Texture Analyzer) with the position of the arm along mode 1 (according to the dimensionally-reduced videofluoroscope analysis). We used a cross-correlation algorithm in MATLAB to correlate timing of these two waves and synchronize the TA and fluoroscopy datasets.

Additionally, 1 mL of 20 weight per volume% aqueous barium sulfate was orally coadministered to provide radiopaque contrast within the lumen of the GI. Contrast provides direct visualization of the lumen of the intestinal segment in real time. In this way, we can distinguish if the magnetic pill has been localized in the intestinal region of interest as compared to the stomach or large intestines, which have different and identifiable lumen morphologies.

X-Ray Verification of Magnetic Localization. Six 600–800 g, male, albino Sprague-Dawley rats underwent localization of a model magnetic pill for a period of 12 h. All rats had access to food and water ad libitum within their acrylic restraint tubes and were handled in accordance with NIH and Institutal Animal Care and Use Committee (IACUC) guidelines. X-rays were taken prior to the start of and after 12 h of magnetic localization to test the efficacy of magnetic capture. All subjects showed magnetic intestinal retention for 12 h.

In Vitro Intermagnetic Force Testing. A cylindrical NIB magnet identical to the orally dosed magnets was affixed by cyanoacrylate glue to a nonmagnetic aluminum pedestal ($\Phi = 1.6$ mm, length $= 1.6$ mm, KJ Magnetics). The cylindrical external NIB magnet ($\Phi = 25$ mm, length $= 25$ mm, KJ Magnetics) was then brought towards the immobilized magnet while monitoring intermagnetic force and separation distance. The in vitro force as a function of distance curve was compared with the in vivo experiments, in which the intermagnetic distance is calculated from tracking the location of the internal and external magnets from biplanar fluoroscopic videos. Intermagnetic force as a function of distance was shown to be negligibly different between the in vitro and in vivo cases. Therefore in vitro intermagnetic force as a function of magnet separation testing can be used to predict if a pair of internal and external magnets will retain an orally administered magnetic pill given the dimensions of the subject and an estimate of the local, propulsive GI forces experienced during digestion.

Histology. Intestinal tissue samples from three rats were recovered post mortem in the region of magnetic retention and 2 cm distal to the region of magnetic retention. Sections were fixed in paraformaldehyde, imbedded in paraffin, sectioned, and stained with hemotoxylin and eosin. Sections were imaged on a Zeiss Axiovert 200 M motorized inverted microscope equipped with an AxioCam MRc5 color camera (Zeiss). Intestinal tissue at the site of localization showed no difference in mechanical integrity or signs of inflammation from distal control samples indicating that the method of magnetic retention has no immediate untoward effects on the intestinal tissue under the reported testing conditions.

Conclusions

Magnetically localized pills serve as a platform technology for addressing a broad array of issues facing the implementation of disease therapies. In particular, therapeutics exhibiting optimal absorption within a limited region of the GI and those therapies that target GI ailments have immediate potential for exploration by using our system and guidelines for magnetic pill retention. Our technique is readily applicable to investigating the therapeutic benefit of prolonged local delivery of NAW therapeutics (e.g., acyclovir, bisphosphonates, furosemide, levodopa, and metformin) at their sites of greatest absorption (1, 3). Additionally, localized oral delivery of polymer nanoencapsulated proteins within specific regions of the GI, genes, and antibodies within the small intestines demonstrated tremendous potential to enable conversion to oral delivery of biologic therapies currently delivered by injection (5, 15–19). Similarly, localized oral delivery to the ileum would expose vaccines to GALT increasing their contact with the immune system (1, 14).

Another avenue for the application of magnetic pill localization is the treatment of GI pathophysiologies including esophageal, gastric, intestinal, and colorectal cancers (2, 7, 9, 10, 13). Magnetic localization of chemotherapeutics at the site of GI tumors, which are simultaneously identifiable on X-ray following intravenous administration of radioopaque contrast, would enable localized dosing while minimizing side effects associated with systemic administration (2, 10). Finally, magnetically localized oral delivery of therapeutics for GI diseases including severe cases of Crohn's disease and acid reflux enables administration directly at the affected site without requiring direct visualization of the pathophysiology in question (1, 10). With the site-specificity of localization confirmed by biplanar videofluoroscopy, magnetic retention could also have use in manipulating pill-based devices such as the PillCam to thoroughly investigate a particular region of interest within the GI (29), or to direct GI tumor ablative therapies noninvasively (30). Safe and effective, monitored magnetic pill localization is a crucial step for investigating and producing new, site-specific therapies for the treatment of a wide range of diseases. With a safe and effective means of localizing pills, the therapeutic value of locally delivered drugs can be assessed in vivo towards the improvement of existing products and the development of new, more effective pharmacotherapies and ingestible devices.

ACKNOWLEDGMENTS. We thank Professor Elizabeth L. Brainerd for her advice on fluoroscope technique and tissue mechanics, Marc Johnson for his assistance with Texture Exponent programming, and Paula Weston for her help with histology. We also thank the funding support of Brown University.

1. Davis SS (2005) Formulation strategies for absorption windows. *Drug Discov Today* 10:249–257.

2. Polyak B, Friedman G (2009) Magnetic targeting for site-specific drug delivery: applications and clinical potential. *Expert Opin Drug Del* 6:53–70.

3. Groning R, Berntgen M, Georgarakis M (1998) Acyclovir serum concentrations following peroral administration of magnetic depot tablets and the influence of extracorporeal magnets to control gastrointestinal transit. *Eur J Pharm Biopharm* 46:285–291.
4. Chen HM, Langer RS (1997) Magnetically-responsive polymerized liposomes as potential oral delivery vehicles. *Pharm Res* 14:537–540.
5. Cheng J, et al. (2006) Magnetically responsive polymeric microparticles for oral delivery of protein drugs. *Pharm Res* 23:557–564.
6. Arruebo M, Fernandez-Pacheco R, Ibarra MR, Santamaria J (2007) Magnetic nanoparticles for drug delivery. *Nano Today* 2:22–32.
7. Ito R, Machida Y, Sannan T, Nagai T (1990) Magnetic granules: a novel system for specific drug delivery to esophageal mucosa in oral administration. *Int J Pharm* 61:109–117.
8. Teply BA, et al. (2008) The use of charge-coupled polymeric microparticles and micromagnets for modulating the bioavailability of orally delivered macromolecules. *Biomaterials* 29:1216–1223.
9. Widder KJ, Morris RM, Poore G, Howard DP, Jr, Senyei AE (1981) Tumor remission in Yoshida sarcoma-bearing rats by selective tartgeting of magnetic albumin microspheres containing doxorubicin. *Proc Natl Acad Sci USA* 78:579–581.
10. Langer R (1998) Drug delivery and targeting. *Nature* 392(Suppl. S):5–10.
11. World Health Organization Fact Sheet 297.
12. National Institute of Diabetes and Digestive and Kidney DiseasesEverhart JE, ed. (2008) *The burden of digestive diseases in the United States* (U.S. Dept of Health and Human Services).
13. Cao Y, Langer R (2010) Optimizing the delivery of cancer drugs that block angiogenesis. *Science Translational Medicine* 2:15ps3.
14. Chen H, Langer R (1998) Oral particulate delivery: status and future trends. *Adv Drug Deliver Rev* 34:339–350.
15. Goldberg M, Gomez-Orellana I (2003) Challenges for the oral delivery of macromolecules. *Nat Rev Drug Discov* 2:289–295.
16. Mathiowitz E, et al. (1997) Biologically erodable microsphères as potential oral drug delivery systems. *Nature* 386:410–414.
17. Gref R, et al. (1994) Biodegradable long-circulating polymeric nanospheres. *Science* 263:1600–1603.
18. Langer R (1990) New methods of drug delivery. *Science* 249:1527–1533.
19. Whitehead K, Shen ZC, Mitragotri S (2004) Oral delivery of macromolecules using intestinal patches: applications for insulin delivery. *J Control Release* 98:37–45.
20. Edelman ER, Mathiowitz E, Langer R, Klagsbrun M (1991) Controlled and modulated release of basic fibroblast growth factor. *Biomaterials* 12:619–626.
21. Brainerd EL, et al. (2010) X-ray reconstruction of moving morphology (XROMM) : précision, accuracy and applications in comparative biomechanics research. *J Exp Zool* 313A:262–279.
22. Hedrick TL (2008) Software techniques for two- and three-dimensional kinematic measurements of biological and biomimetic systems. *Bioinspir Biomim* 3:6.
23. Riskin DK, et al. (2008) Quantifying the complexity of bat wing kinematics. *J Theor Biol* 254:604–615.
24. Guignet R, Bergonzelli G, Schlageter V, Turini M, Kucera P (2006) Magnet tracking : a new tool for in vivo studies of the rat gastrointestinal motility. *Neurogastro and Mot* 18:472–478.
25. Laulicht B, Tripathi A, Schlageter V, Kucera P, Mathiowitz E (2010) Understanding gastric forces calculated from high-resolution pill tracking. *Proc Natl Acad Sci USA* 107:8201–8206.
26. Chong LD (2010) Physiology: easy to swallow, hard to digest. *Science* 328:5979.
27. De S, et al. (2007) Assessment of tissue damage due to mechanical stresses. *The International Journal of Robotics Research* 26:1159–1171.
28. Ferens DM, et al. (2005) Motor patterns and propulsion in the rat intestine in vivo recorded by spatio-temporal maps. *Neurogastroent and Motil* 17:714–720.
29. Iddan G, Meron G, Glukhovsky A, Swain P (2000) Wireless capsule endoscopy. *Nature* 405:417.
30. Kennedy JE (2005) High-intensity focused ultrasound in the treatment of solid tumors. *Nat Rev Cancer* 5:321–327.